# Cribs to 3A1, 2009

Jie Li

**Crib 1**

(a) Compex potential

$$F(z) = Uz + \frac{i\Gamma}{2\pi}\ln(z - ia) - \frac{i\Gamma}{2\pi}\ln(z + ia) \tag{1}$$

(b) Stagnation points

$$\frac{dF}{dz} = U + \frac{i\Gamma}{2\pi}\left(\frac{1}{z - ia} - \frac{1}{z + ia}\right) \tag{2}$$

$$= U + \frac{i\Gamma}{2\pi}\frac{2ia}{z^2 + a^2} = \frac{U(z^2 + a^2) - \Gamma a/\pi}{z^2 + a^2} = 0 \tag{3}$$

$$U(z^2 + a^2) - \frac{\Gamma a/\pi}{z^2 + a^2} = 0 \tag{4}$$

$$z = \pm\sqrt{\Gamma a/\pi U - a^2} \tag{5}$$

(c)

$$F(z) = Uz + \frac{i\Gamma}{2\pi}\ln(z - ia) - \frac{i\Gamma}{2\pi}\ln(z + ia) \tag{6}$$

$$= Uz + \frac{i\Gamma}{2\pi}\ln(z(1 - ia/z)) - \frac{i\Gamma}{2\pi}\ln(z(1 + ia/z)) \tag{7}$$

$$= Uz + \frac{i\Gamma}{2\pi}(\ln(z) + \ln(1 - ia/z)) - \frac{i\Gamma}{2\pi}(\ln(z) + \ln(1 + ia/z)) \tag{8}$$

$$= Uz + \frac{i\Gamma}{2\pi}(-ia/z - ia/z) = Uz + \frac{\Gamma a}{\pi z} = Uz + \frac{C}{\pi z} \tag{9}$$

(d)

(i)

$$F(z) = Uz + \frac{C}{\pi z} \tag{10}$$

$$\frac{dF}{dz} = U - \frac{C}{\pi z^2} = 0 \tag{11}$$

$$z = \pm\sqrt{\frac{C}{\pi U}} \tag{12}$$

(ii) This flow is uniform flow + a doublet wiht strenght $2C$. As known from the lecture, it can be used to model a flow over a cylinder with radius $\sqrt{\frac{C}{\pi U}}$.

(iii) Flow pattern inside and outside the cylinder, see figure 1.

**Crib 2**

(a)

$$F(z) = Uz + \frac{m}{2\pi}\ln(z) \tag{13}$$

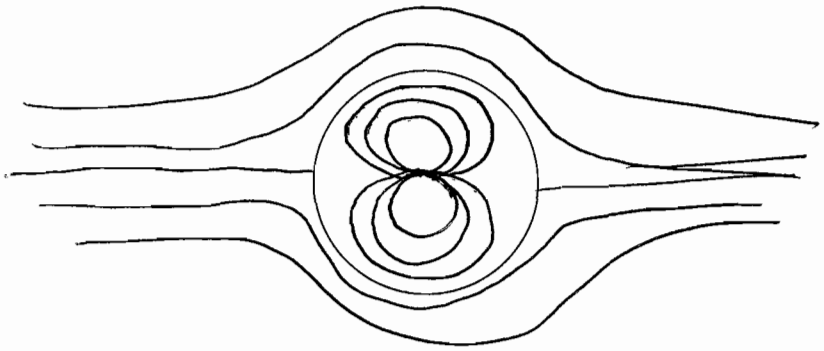

Figure 1: Flow pattern inside and outside the cylinder.

(b)

$$\phi + i\psi = U(x + iy) + \frac{m}{2\pi}(\ln(r) + i\theta) \tag{14}$$

$$\psi = Uy + \frac{m\theta}{2\pi} = 1 \tag{15}$$

Far upstream $x \to -\infty$, $\theta \to \pi$

$$\psi = Uy + \frac{m\pi}{2\pi} = 1 \Rightarrow y(-\infty) = \frac{1 - m/2}{U} \tag{16}$$

Far upstream $x \to \infty$, $\theta \to 0$

$$\psi = Uy + \frac{m \times 0}{2\pi} = 1 \Rightarrow y(\infty) = \frac{1}{U} \tag{17}$$

$$\Delta y = y(\infty) - y(-\infty) = \frac{m}{2U} \tag{18}$$

(c) To find the pressure use Bernoulli. So find the velocity
Far upstream the velocity is simply $U$.

$$u - iv = \frac{dF}{dz} = U + \frac{m}{2\pi z} \tag{19}$$

At our point of interest $x = 0$, but what is $y$

$$\theta = \pi/2, \quad Uy + \frac{m\pi/2}{2\pi} = 1 \tag{20}$$

$$y = \frac{1 - m/4}{U} \tag{21}$$

At $z = x + iy = \frac{1-m/4}{U} i$,

$$u - iv = U + \frac{m}{2\pi z} \Rightarrow u^2 + v^2 = U^2 + \left(\frac{m}{2\pi(1 - m/4)}\right)^2 U^2 \tag{22}$$

Bernoulli equation:

$$P_\infty + \frac{1}{2}\rho U^2 = P + \frac{1}{2}\rho\left(U^2 + \left(\frac{m}{2\pi(1-m/4)}\right)^2 U^2\right) \tag{23}$$

$$\frac{P_\infty - P}{\frac{1}{2}\rho U^2} = \left(\frac{m}{2\pi(1-m/4)}\right)^2 \tag{24}$$

**Crib 3**

(a) Flux at bubble surface:

$$4\pi R^2 \frac{dR}{dt}$$

flux at radius $r$

$$4\pi r^2 u$$

Mass conservation

$$4\pi R^2 \frac{dR}{dt} = 4\pi r^2 u \Rightarrow u = \frac{R^2}{r^2}\frac{dR}{dt}$$

Potential

$$\phi = --\int_r^\infty u dr = -\frac{R^2}{r}\frac{dR}{dt}$$

(b)

$$\frac{\partial \phi}{\partial t} = -\frac{2R(\frac{dR}{dt})^2 + R^2\frac{d^2R}{dt^2}}{r}$$

At $r = +\infty$, $\phi = 0$, $u = 0$,
at $r = R$,

$$\frac{\partial \phi}{\partial t} = -2(\frac{dR}{dt})^2 + R\frac{d^2R}{dt^2}$$

$$u = \frac{dR}{dt}$$

From Bernoulli equation,

$$-2(\frac{dR}{dt})^2 + R\frac{d^2R}{dt^2} + \frac{1}{2}(\frac{dR}{dt})^2 + \frac{p_b}{\rho} = \frac{p_\infty}{\rho}$$

$$R\frac{d^2R}{dt^2} + \frac{3}{2}(\frac{dR}{dt})^2 = \frac{p_b}{\rho} - \frac{p_\infty}{\rho} \tag{25}$$

(c)

$$R = a + x, \quad \frac{dR}{dt} = \frac{dx}{dt}, \quad \frac{d^2R}{dt^2} = \frac{d^2x}{dt^2}$$

$$p_b = KR^{-3\gamma} = K(a+x)^{-3\gamma} = Ka^{-3\gamma}(1+x/a)^{-3\gamma} \approx p_\infty(1-3\gamma x/a)$$

From the governing equation (25),

$$(a+x)\frac{d^2x}{dt^2} + \frac{3}{2}(\frac{dx}{dt})^2 = \frac{1}{\rho}\left(p_\infty\left(1-3\gamma x/a\right) - p_\infty\right)$$

Neglect non-linear terms,

$$a\frac{d^2x}{dt^2} + \frac{3\gamma p_\infty}{\rho a}x = 0. \tag{26}$$

The frequency of the oscillation is

$$(\frac{3\gamma p_\infty}{\rho})^{1/2}/a,$$

proportional to $1/a$.

**Crib 4**

(a)

$$\frac{U}{U_\tau} = \frac{1}{\kappa}\ln\left(\frac{yU_\tau}{\nu}\right) + C$$

Take the derivative with respect to y,

$$\frac{\partial U}{\partial y} = \frac{U_\tau}{\kappa y} = 100$$

$$U_\tau = 100 \times 0.4 \times 0.03 = 1.2\ m/s$$

$$C_f = \frac{\tau_w}{1/2\rho U_1^2} = \frac{\rho U_\tau^2}{1/2\rho U_1^2} = \frac{2U_\tau^2}{U_1^2} = 0.00222$$

(b)

$$\frac{U}{U_\tau} = \frac{1}{\kappa}\ln\left(\frac{yU_\tau}{\nu}\right) + C$$

At the edge

$$\frac{U_1}{U_\tau} = \frac{1}{\kappa}\ln\left(\frac{\delta U_\tau}{\nu}\right) + C$$

$$Re = \frac{\delta U_\tau}{\nu} = e^{\kappa\frac{U_1}{U_\tau} - C} = e^{.4\times 25} = 22026$$

(c) Velocity gradient at the wall

$$\mu\left(\frac{\partial U}{\partial y}\right)|_{y=0} = \tau_w = \rho U_\tau^2$$

$$\left(\frac{\partial U}{\partial y}\right)|_{y=0} = \frac{U_\tau^2}{\nu} = \frac{1.2^2}{1.5\times 10^{-5}} = 96000\ 1/s$$

(d) von Karman momentum integral equation

$$\frac{d\theta}{dx} + \frac{H+2}{U_1}\theta\frac{dU}{dx} = \frac{C_f}{2}$$

$$U_1\frac{dU}{dx} = -\frac{1}{\rho}\frac{dp}{dx}$$

$$\frac{H+2}{\rho U_1^2}\theta\frac{dp}{dx} = \frac{d\theta}{dx} - \frac{C_f}{2} = 0.0111 - 0.00111 = 0.00999$$

$$\frac{dp}{dx} = \frac{0.00999\rho U_1^2}{(H+2)\theta}$$

**Crib 5**

(a) (i)

$$\delta^* = \int_0^\infty 1 - \frac{U}{U_1}dya\int_0^\delta 1 - \left(\frac{y}{\delta}\right)^2 dy = \frac{2}{3}\delta$$

(ii)

$$\delta^* = \int_0^\infty (1 - \frac{U}{U_1})\frac{U}{U_1}dy = \frac{2}{15}\delta$$

(iii)

$$H = \delta^*/\theta = 5$$

(vi)

$$\tau_w = \mu\frac{\partial U}{\partial y}|_{y=0} = \frac{2U_1 y}{\delta^2}|_{y=0} = 0$$

$$C_f = 0.$$

(b) von Karman momentum integral equation

$$\frac{d\theta}{dx} + \frac{14}{15U_1}\theta\frac{dU}{dx} = 0$$

$$\frac{2}{15}\frac{d\delta}{dx} + \frac{14}{15U_1}\theta\frac{dU}{dx} = 0$$

$$\frac{7}{U_1}\frac{dU}{dx} = -\frac{1}{d\delta}\frac{d\delta}{dx}$$

$$U = A\delta^{-1/7}\ A \text{ is a constant}$$

(d) outside the BL

$$U_1\frac{dU}{dx} = -\frac{1}{\rho}\frac{dp}{dx}$$

inside the BL

$$-\frac{1}{\rho}\frac{dp}{dx} + \nu\frac{\partial^2 u}{\partial y^2}$$

$$\frac{\partial^2 u}{\partial y^2} = \frac{2U_1}{\delta^2}$$

$$\frac{dU}{dx} = -\frac{2\nu}{\delta^2}$$

Because

$$U = A\delta^{-1/7}$$

$$\delta^{\frac{6}{7}}\frac{d\delta}{dx} = 14\nu A$$

$$\frac{7}{13}\frac{d}{dx}\left(\delta^{\frac{13}{7}}\right) = 14\nu A$$

$$\delta = (26\nu A x)^{\frac{7}{13}},$$

where we have used $\delta = 0$ at $x = 0$.

Finally,

$$U = Bx^{-\frac{1}{13}},\ B \text{ is a constant}$$

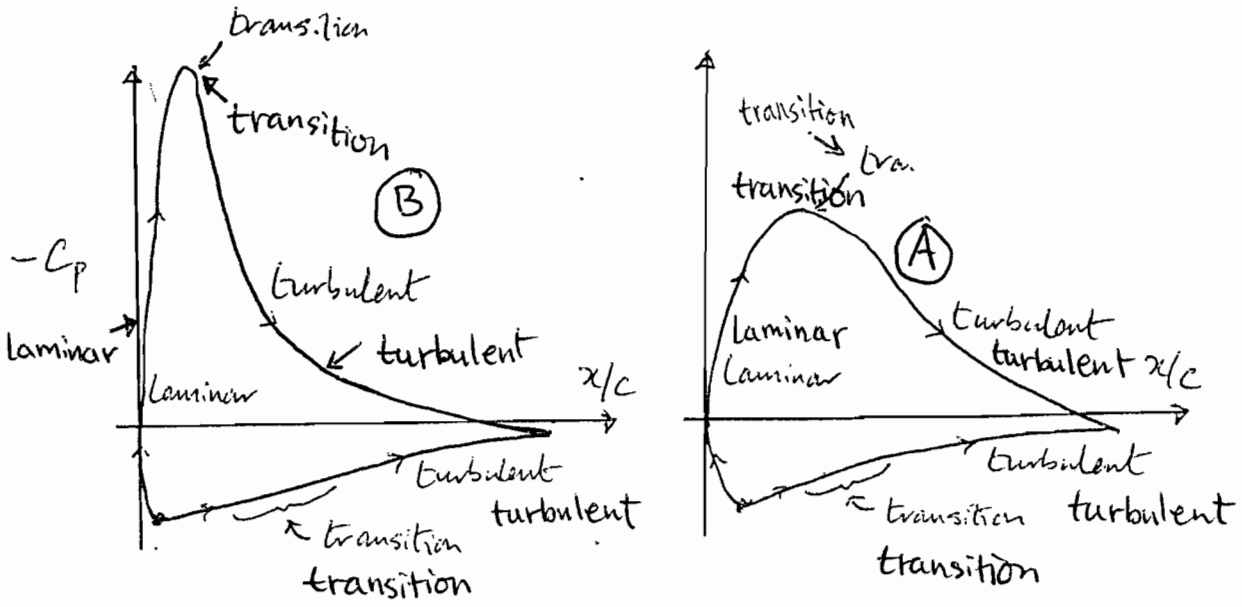


Figure 2: Pressure coefficient distributions at highly super-critical regime.

**Crib 7**

(a)

- Aerofoil $B$ has different pressures on upper and lower surfaces while Aerofoil $A$ does not *Rightarrow* $B$ is cambered, $A$ is symmetrical.
- Adverse pressure gradients (APGs) on second half of upper surface are much lower for $B$ *Rightarrow* $B$ is thin (6%), $A$ is thck (24%)

(b) (i)

Key differences, $B$ cf $A$ (see figure 2):

- narrower, higher suction peak.
- weaker upper surface APGs towards trailing edge (T.E.)

(ii) Qualitative boundary layer (BL) same for both aerofoils,

- **Upper surface**: BL stays laminar in favorable pressure gradient from stagnation point to suction peak, then undergoes natural transition at, soon after, onset of APGs, (could also mention possibility of transition via separation/reattachment, as long as it's made clear that separation bubble is very short, and does not affect $C_p$ distribution.)
- **Lower surface**: pressure gradient is favorable from stagnation point to T.E., but magnitude of Reynolds number means that natural transition is likely at some point.

(iii)

- **Aerofoil** $B$: Strong APG after suction peaks means leading edge (L.E.) stall most likely; lift increases almost linearly with incidence until stall angle, beyond which it drops suddenly, with a large corresponding drag increase. Little can be done about this without altering the section geometry.

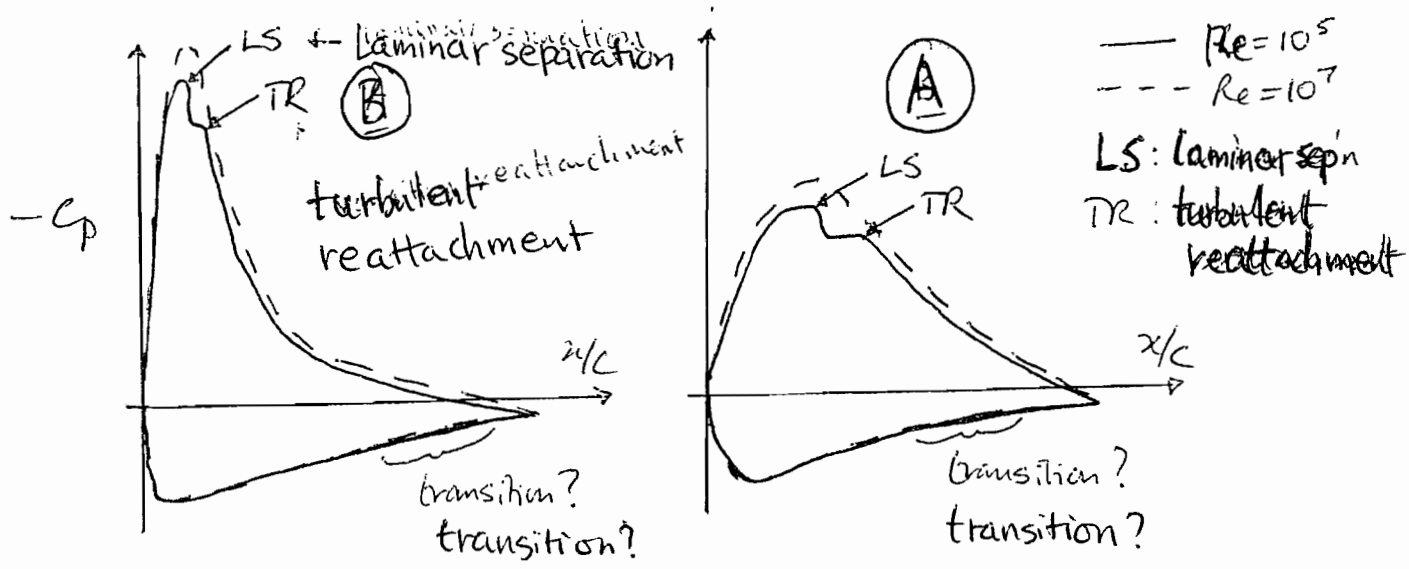


Figure 3: Pressure coefficient distributions at critical regime.

- **Aerofoil** *A*: BL unlikely to separate immediately after suction peak, but will eventually succumb to cumulative effect of upper surface APGs: trailing edge stall. Lift increase with incidence tails off towards stall, after which it deceases gradually. Drag increases continuously. Improvement may be possible by promoting BL mixing towards T.E. with vortex generators.

(c)

(i) (see figure 3)

- **Main points**: upper surface transition will now occur via laminar separation/turbulent reattachment, and presence of separation bubbles will be evident in surfaces pressures. Lower surface transition will be later, and may not occur at all.

- **Subtle points**: slight reduction of lift due to increased BL thicknesses.

(ii) Still expect L.E. stall (via "bubble burst") for *B* and T.E. stall for *A*. It might now be possible to delay *B* 's stall slightly by forcing transition to turbulence (e.g. with 'turbulator') just before the LS point.

Q7

c)(i)

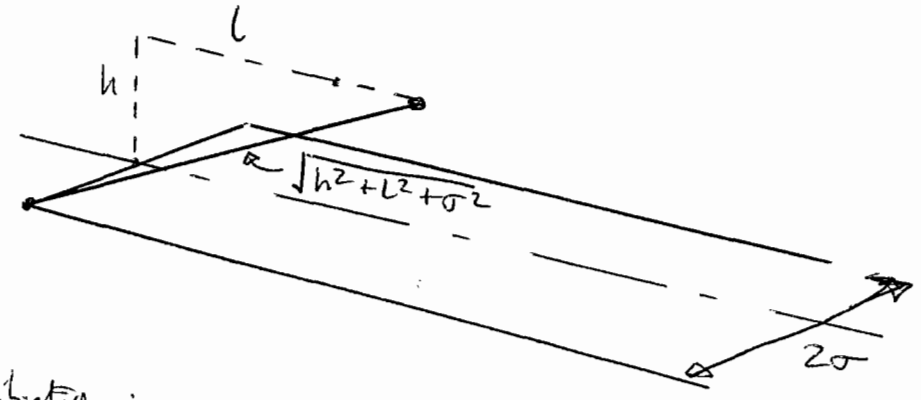


Leg contribution:

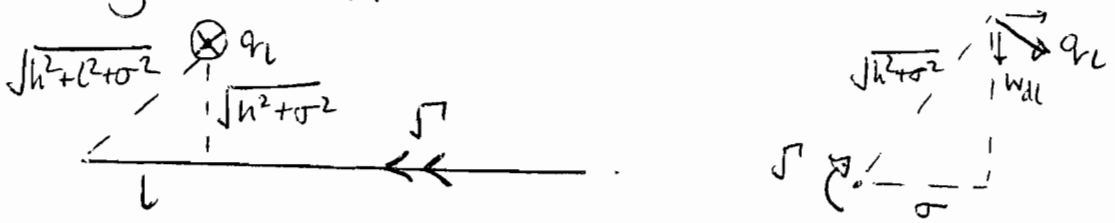


Biot-Savart $\Rightarrow$ $$q_l = \frac{\Gamma}{4\pi\sqrt{h^2+\sigma^2}}\left[1+\frac{l}{\sqrt{h^2+l^2+\sigma^2}}\right]$$

$$w_{dl} = q_l \frac{\sigma}{\sqrt{h^2+\sigma^2}} = \frac{\Gamma}{4\pi}\frac{\sigma}{h^2+\sigma^2}\left[1+\frac{l}{\sqrt{h^2+l^2+\sigma^2}}\right]$$

Head contribution:

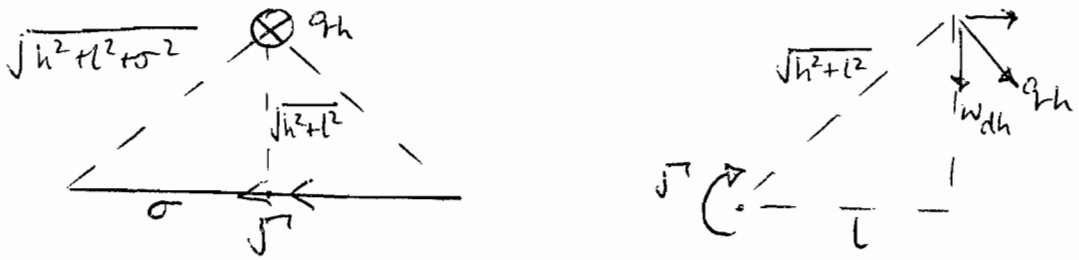


$$q_h = \frac{\Gamma}{2\pi\sqrt{h^2+l^2}}\frac{\sigma}{\sqrt{h^2+l^2+\sigma^2}}$$

$$w_{dh} = q_h \frac{l}{\sqrt{h^2+l^2}} = \frac{\Gamma}{2\pi}\frac{l}{h^2+l^2}\frac{\sigma}{\sqrt{h^2+l^2+\sigma^2}}$$

$$w_d = 2w_{dl} + w_{dh} = \frac{\Gamma\sigma}{2\pi}\left\{\frac{1}{h^2+\sigma^2} + \frac{l}{\sqrt{h^2+l^2+\sigma^2}}\left[\frac{1}{h^2+\sigma^2}+\frac{1}{h^2+l^2}\right]\right\}$$

(ii) At $l=0$ $w_d = \frac{\Gamma\sigma}{2\pi}\frac{1}{h^2+\sigma^2}$, half of that far downstream.

(iii) As the downwash includes an odd function of $l$, one wing will experience more than the other, inducing a rolling moment, and hence acceleration, on the aircraft.

a) Horseshoe vortex model:

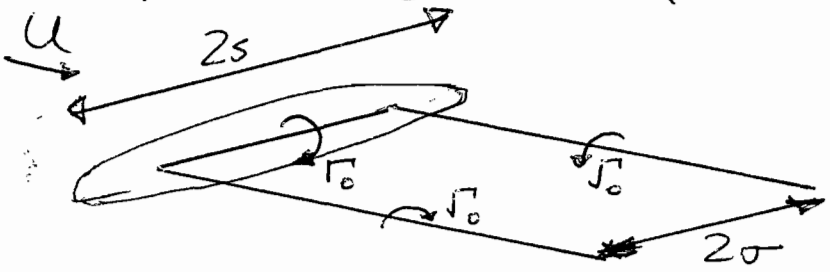


Lift-distribution:

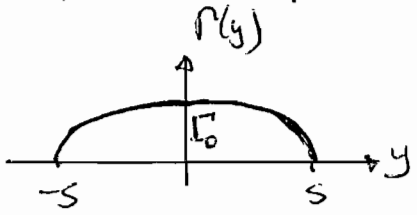


The horseshoe vortex lumped-parameter model consists of a head section, length 2σ, sitting on the wing ¼-chord line, and two legs, extending from the ends of the head to infinity in the streamwise direction. Its strength is equal to the wing-root circulation and its semi-width σ is πs/4, where s is the wing semi-span.

b) (i) Far downstream, we need only consider the legs:

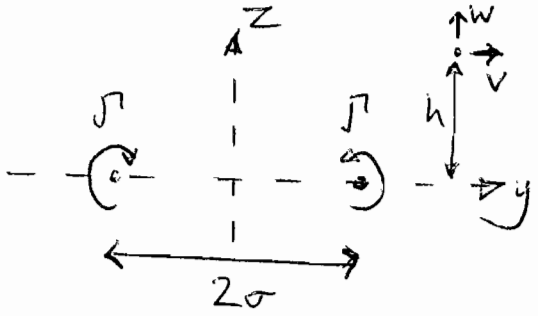


$$w_d = -w = -\frac{\Gamma}{2\pi}\left[\frac{y-\sigma}{(y-\sigma)^2+h^2} - \frac{y+\sigma}{(y+\sigma)^2+h^2}\right]$$

(ii) Downwash changes angle of attack:

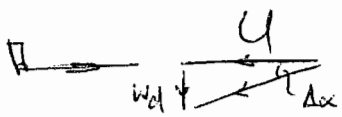


Consider how downwash varies with y:

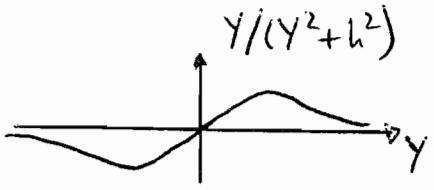


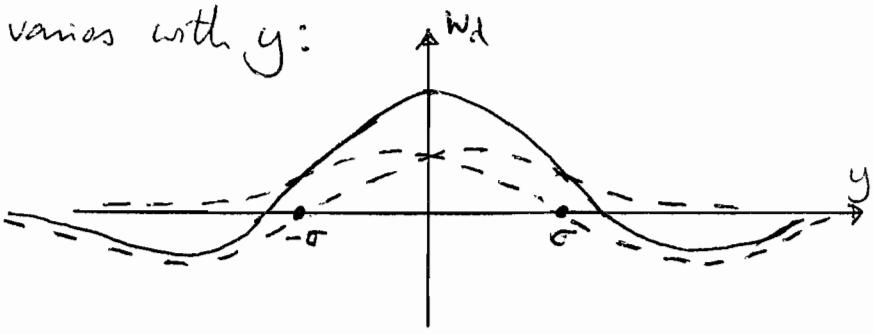


So the aircraft experiences, successively, an increase, decrease and increase in angle of attack, with associated upwards, downwards and upwards accelerations.

Crib Q8

a) There is not enough space for a closed-return wind tunnel. An open-return tunnel with a 9:1 contraction, a 1m long working section and a 10m long diffuser would fit into the 20m space, allowing for air to circulate into and out of the tunnel at either end. For best flow quality and simplicity of design, a suction-type tunnel with a closed working section would be best.

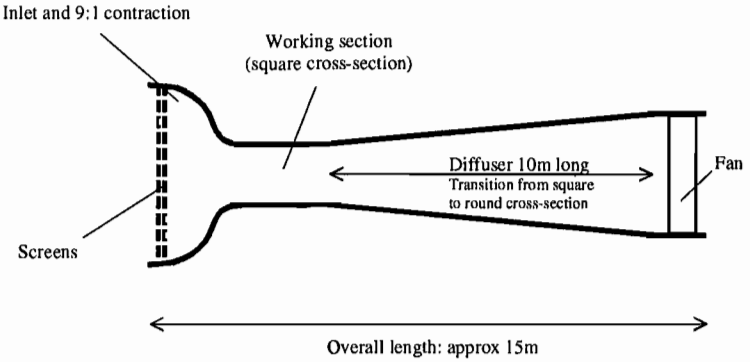


b) A good estimate for the diffuser included angle would be 5deg (to ensure that separation is avoided). To get an estimate for the area change we can for now assume that the cross-section remains square (in reality this would transition to round but the effective area would be similar). The exit area is thus:

$A_x=[H_{ws}+2L\tan 2.5°]^2$ , where $H_{ws}$ is the working section height (1m) and L=10m

$A_x=3.5m^2$

The exit velocity is thus

$U_x=U_{ws}\ A_{ws}/A_x$

The fan power is equivalent to the power in the exhaust jet (excluding losses):

$P_x=1/2\ ro\ U_x^3\ A_x$

Equating the above to 10kW, assuming ro=1.225 kg/m$^3$ (compressibility can be ignored) gives:

$U_x=16.7m/s$

The power factor of the wind tunnel is 0.08 (proportional to square of area ratio $A_{ws}/A_x$), showing that the use of a diffuser makes a big difference to the power consumption.

c) The main losses are likely to be:

Fan losses
Losses due to grid drag ahead of contraction (and flow straighteners if used)
Wall friction
Model drag (if model is placed in working section)

d) see lecture notes. Briefly:

LDA:
- high spatial resolution
- good/excellent time (frequency) resolution up to 10s of kHz
- less stringent seeding requirements than PIV
- only measures in one location – needs traversing to sample whole flowfield
- best for steady/quasi-steady flows if more than one location is to be measured

PIV:
- can measure large domain simultaneously
- needs excellent seeding quality
- spatial resolution depends on camera and magnification (typically less good than LDA)
- slower: max frequency of order of 1kHz (typically only 10s of Hz)

e) LDA: turbulent boundary layer profile, traversing measurement volume across the flow
PIV: unsteady wake flow

# Numerics Answers

Jie Li

Question 4,

(a) $U_\tau = 1.2\ m/s$, $C_f = 0.00222$.

(b) $Re = 22026$.

(c) $\left(\frac{\partial U}{\partial y}\right)|_{y=0} = 96000\ 1/s$.

Question 8,

(b) $U_{\text{exit}} = 16.7$ m/s, $U_{\text{worksection}} = 58.45$ m/s. Power factor 0.08.